sciendo
ISSN 2083-1587; e-ISSN 2449-5999
2025,Vol. 29,No.1, pp. 63-78
Agricultural Engineering
https://agriceng.org
DOI: 10.2478/agriceng-2025-0005

MATHEMATICAL MODEL OF THIN LAYER DRYING OF PURPLE YAM BY INFRARED ASSISTED HEAT PUMP DRYING

Le Anh Duc[a], Nguyen Hay[b], Pham Van Kien[c,*], Nguyen Thanh Tan[c], Dang Quoc Cuong[d]

[a] Nong Lam University, Ho Chi Minh City, Vietnam, e-mail: leanhduc@hcmuaf.edu.vn, ORCID 0000-0002-8498-6203
[b] Faculty of Vehicle and Energy Engineering, University of Technology and Education Ho Chi Minh City, Vietnam, e-mail: ng.hay@hcmuaf.edu.vn, ORCID 0000-0002-4068-9362
[c] Faculty of Automotive Engineering, School of Technology, Van Lang University, Ho Chi Minh City, Vietnam, e-mail: kien.pv@vlu.edu.vn; ORCID 0000-0002-0974-0908; tan.nguen@vlu.edu.vn; ORCID 0009-0001-6353-1621
[d] Faculty of Engineering and Technology, Nguyen Tat Thanh University, Ho Chi Minh City, Vietnam, e-mail: dqcuong@ntt.edu.vn, ORCID 0000-0002-7809-2107

Corresponding author: e-mail: kien.pv@vlu.edu.vn

ARTICLE INFO

Article history:
Received: December 2024
Received in the revised form: March 2025
Accepted: April 2025

Keywords:
drying rate;
heat pump;
effective moisture diffusivity;
activation energy;
drying temperature;
IR power

ABSTRACT

This study focused on the thin-layer drying of yam by infrared-assisted heat pump drying to determine the thin-layer drying model, the effective moisture diffusivity, and the activation energy of moisture within the yam. The thin-layer drying experiment was conducted with input drying parameters such as drying temperatures of 40, 45, and 50°C, drying air velocity of 2.5 m·s⁻¹, and infrared power of 250, 300, and 350 W. In order to determine a suitable thin-layer drying model for describing the yam drying process, six different thin-layer drying models (Lewis, Page, Modified Page, Henderson and Pabis, Wang and Singh, and Midilli) were chosen for nonlinear regression with the experimental drying data. The Midilli model was found to be the most suitable drying model for describing the thin-layer drying of yam. The average effective moisture diffusivity was in the range of 4.184×10^{-9} to 8.142×10^{-9} m²·s⁻¹, and the activation energy was in the range of 16.78 to 21.01 kJ·mol⁻¹ over the proposed range of drying input parameters

Introduction

Yam is one of the most popular agricultural products in many tropical countries such as Burkina Faso, Ghana, Togo, Nigeria, and Vietnam. There are more than 600 different types of yam, among which purple yam, yellow yam, and water yam are widely used for food purposes (Olatoye and Arueya, 2019). Yam contains many nutrients including starch, proteins, lipids, minerals, vitamin C, and carbohydrates, which are beneficial to human health (Kai-Nong et al., 2019; Kartik et al., 2023). Fresh yam has a high moisture content in the range of 50–80% (w.b.), which stimulates bacterial activity. Thus, fresh yam spoils easily after harvest, and it is also difficult to preserve fresh yam with high moisture content for a long period (Linlin et al., 2019; Nurdi et al., 2021; Ononogbo et al., 2022).

Drying has been an effective method of preserving agricultural products because the drying process reduces the moisture content of agricultural products to a required level and extends the preservation period of the dried products (Abbaspour et al., 2019; Srikanth et al., 2019). Dried yam can be preserved for a long time and used for food processing and starch extraction (Srikanth et al., 2019). Three heat transfer methods, including convection, conduction, and radiation, are applied during the drying process (Liu et al., 2019). Currently, common drying methods include sun drying, heat pump drying, convective hot air drying, vacuum drying, microwave drying, infrared (IR) drying, and hybrid drying (Kaveh et al., 2018). Hot air drying is widely used because of its high drying rate, low equipment cost, and ease of operation. However, high drying temperatures can significantly affect the quality of dried products (Omari et al., 2018). With its low humidity and low air temperature, heat pump drying can maintain the quality of dried products and shorten the process (Fakhreddin, 2021).

In drying techniques using infrared radiation, the IR heating mechanism can enhance the heating rate to reduce drying time and improve the quality of dried products (Fakhreddin et al., 2020; Rastogi et al., 2012; Kien et al., 2024). In IR heating, the drying material is directly affected by electromagnetic radiation through infrared emission, which causes the molecules within the material to vibrate at high frequency. As a result, internal heat is generated within the material due to molecular friction, significantly supporting the heating rate (Fasina et al., 2001; Salam, 2019; Zi et al., 2022; Dan et al., 2021). Hybrid drying, which combines IR with other drying methods such as hot air or heat pump drying, has proven to be an effective method for drying agricultural products, improving both drying rate and the quality of dried products (Onwude et al., 2019; Qu et al., 2019; Wu et al., 2019).

There have been previous studies on yam drying to evaluate the efficiency of various methods, especially in terms of drying rate, drying time, nutritional content, color, and surface quality of the dried products (Chineze et al., 2020; Adebimpe et al., 2021; Nurdi et al., 2021; Ononogbo et al., 2022). The results showed that input drying parameters, including drying temperature, air velocity, and drying method, primarily determined the effectiveness of the yam drying process.

The drying process consists of two main stages: the constant rate period and the falling rate period (Nidhal, 2018). During the constant rate period, the drying rate remains almost constant at a high level. Moreover, the temperature of the drying material increases slowly because most of the supplied heat is used for vaporization. The falling rate period begins when the moisture content reaches the critical level. In this stage, the drying rate is lower and continues to decrease until the moisture content reaches equilibrium. At this point, the drying process ends. The drying process involves a complex mechanism of simultaneous heat and mass transfer (Uwem et al., 2009; Waheed and Komolafe, 2019; Le et al., 2023).

Previous studies on experimental thin-layer drying have aimed to determine the effective moisture diffusivity and activation energy of moisture within the drying material. Waheed and Komolafe (2019) studied the drying kinetics of cocoa beans at temperatures of 40, 50, and 60°C. The effective moisture diffusivity of cocoa beans ranged from 9.9269×10^{-11} to 4.4671×10^{-10} $m^2\cdot s^{-1}$, and the activation energy was 23.61 $kJ\cdot mol^{-1}$. Abhishek et al. (2019) conducted experimental thin-layer drying of radish using a convective hot air drying method at temperatures of 30, 40, and 50°C. The results showed that the effective moisture diffusivity increased from 3.3×10^{-8} to 5.55×10^{-8} m^2 min^{-1} with increasing temperature, and the activation energy was 18.49 kJ·mol^{-1}.

Abhishek et al. (2020) conducted experimental thin-layer drying of beetroot using a convective hot air drying method at temperatures of 70, 75, 80, and 85°C. An increase in temperature led to higher moisture diffusivity values: 3.11×10^{-8}, 3.89×10^{-8}, 4.03×10^{-8}, and 5.48×10^{-8} m^2·min^{-1}, respectively, and the activation energy was 35.59 kJ·mol^{-1}. Soner et al. (2020) studied the drying kinetics of apple using convective hot air, microwave, and ultrasonic power. The results confirmed that effective moisture diffusivity increased significantly in hybrid drying methods. At 50°C, convective hot air drying resulted in a diffusivity of 3.115×10^{-10} m^2·s^{-1}, while microwave-assisted drying at 120, 350, and 600 W resulted in diffusivity values of 3.451×10^{-10}, 5.489×10^{-10}, and 9.765×10^{-10} m^2·s^{-1}, respectively. Ultrasonic-assisted drying at 50 and 100 W gave values of 3.845×10^{-10} and 6.753×10^{-10} m^2·s^{-1}.

John et al. (2020) conducted thin-layer drying of yam slices using a convective hot air dryer. The activation energy ranged from 10.59 to 54.93 kJ·mol^{-1}, while the effective moisture diffusivity increased from 6.382×10^{-9} to 1.641×10^{-7} m^2·s^{-1} with rising temperature and air velocity. Mostafa et al. (2020) performed experimental thin-layer drying of yams with a hot air dryer at 50, 60, 70, and 80°C and an air velocity of 1.5 m·s^{-1}. The results showed that increasing temperature enhanced the drying rate, and effective moisture diffusivity rose from 2.01×10^{-10} to 4.25×10^{-10} m^2·s^{-1}. The drying process occurred entirely in the falling rate period. Egbe (2022) studied the drying kinetics of yam slices at 60, 70, and 80°C using convective hot air. The results confirmed that drying temperature significantly affected the drying rate.

Studying the drying kinetics of thin-layer drying is essential because it clarifies the nature of the process and provides a foundation for improving drying efficiency. Although there have been studies on yam thin-layer drying kinetics, few have investigated the IR-assisted heat pump drying method, which is considered effective for drying agricultural products. The objective of this study was to conduct experimental thin-layer drying of yam slices using an IR-assisted heat pump drying method to determine the most appropriate drying model, the effective moisture diffusivity, and the activation energy of moisture during the drying process.

Materials and Methods

Material

Yam samples used for the thin-layer drying experiment were purple yam. Fresh yam was purchased at Binh Dien Agricultural Market, Ho Chi Minh City, Vietnam. The yam was peeled and sliced to a thickness of 2.5 mm, with an average diameter of 150 mm. Fresh yam had an initial moisture content of 2.82 ± 0.01% (d.b.). Each experimental drying batch used 1,000 g of yam.

Figure 1. Fresh sliced purple yam samples

Experimental Methods

The IR-assisted HP dryer used for the drying experiment is shown in Figure 2 (Kien et al., 2024). The main components of the dryer included a heat pump with a maximum capacity of 0.75 kW, and infrared tubes operating at 50 Hz, with power settings of 250, 300, and 350 W (Onwude et al., 2019; Kien et al., 2024). The working principle of the IR-assisted HP dryer is illustrated in Figure 2. Specifically, drying air was drawn in and circulated through the heat pump unit. The air passed sequentially through the compressor, condenser, expansion valve, and evaporator, reaching the specified temperature, velocity, and humidity before entering the drying chamber. Inside the chamber, infrared radiation combined with the drying air to carry out the drying process.

As noted in previous studies (Le et al., 2023; Kien et al., 2024), experimental IR-assisted HP drying modes for yam were selected within a drying air temperature range of 40-50°C and IR power between 200-350 W. Within these parameter ranges, drying efficiency was significantly improved, with both increased drying rate and enhanced product quality. Therefore, to investigate the kinetics of the thin-layer IR-assisted HP drying process for yam in more detail, the experiments in this study were conducted under the following input conditions: drying air temperatures of 40, 45, and 50°C; air velocity of 2.5 $m \cdot s^{-1}$; and IR power of 250, 300, and 350 W.

The initial moisture content of the yam samples was determined using a moisture analyzer (YOKE DSH-50A-1), with a maximum sample weight of 50 g ± 0.01% and a moisture range of 0-100%.

An electronic scale (OHAUS SPX2202), with a measurement range of 2,200 g ± 0.01 g, was used to weigh the yam samples during the drying process. The weight was recorded every 15 minutes until the samples reached a final moisture content of 0.13 ± 0.01 (d.b.), and all tests were conducted in triplicate.

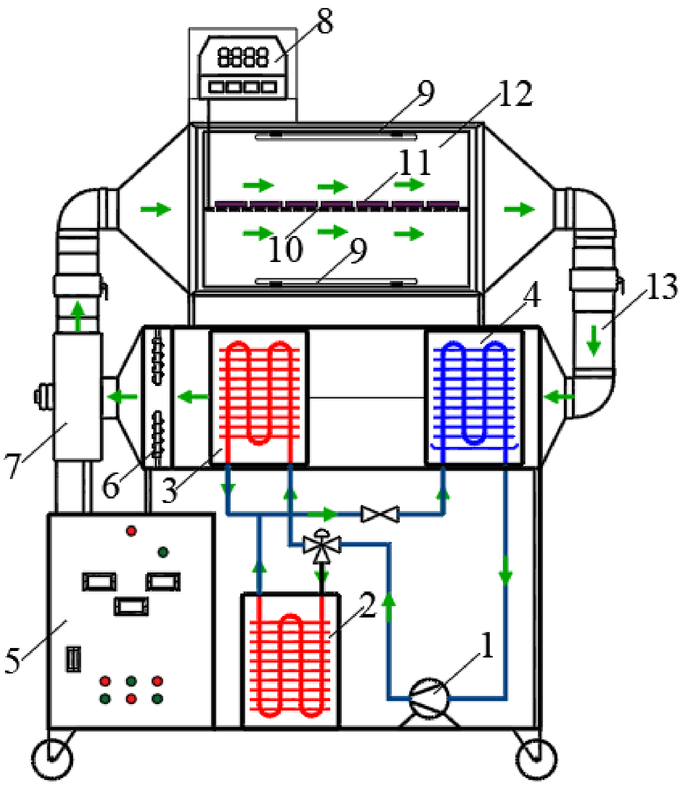

Figure 2. The IR assisted HP dryer model:

Components: 1. Compressor; 2. Condenser; 3. Sub-Condenser 4. Evaporator; 5. Controller unit; 6. Thermistors; 7. air pump; 8. Electronic scale; 9. infrared tubes; 10. Drying tray; 11. Yam sample; 12. Drying chamber; 13. Air pipe

Mathematical Modeling

Thin layer drying model chosen for nonlinear regression with the experimental drying data are given in Table 1 (Royen et al., 2020; Akoy, 2014; Behera et al., 2018; Keneni et al., 2019; Koua et al., 2009; Midilli and Kucuk, 2003).

Moisture content of the drying material was calculated on dry basis (d.b) and the time is calculated in seconds. Moisture ratio (MR) was defined by the equation below:

$$\mathrm{MR} = \frac{M - M_e}{M_i - M_e} \quad (1)$$

where:

M (d.b) is moisture content of drying material at the time τ;
M_e (d.b) is equilibrium moisture content of drying material;
M_i (d.b) is initial moisture content of drying material.

Table 1.
Selected thin-layer drying models.

Model name	Thin layer drying model	References
Lewis	MR = exp(-k.t)	Royen et al. (2020)
Page	MR = exp(-k.t^n)	Akoy (2014)
Modified Page	MR = exp(-k. τ)^n	Behera et al. (2018)
Henderson and Pabis	MR = a.exp(-k. τ)	Keneni et al. (2019)
Wang and Singh	MR = 1 + a. τ + b. τ^2	Koua et al. (2009)
Midilli	MR = a.exp(-k. τ^n) + b. τ	Midilli and Kucuk (2003)

**MR is Moisture ratio; τ is drying time; a, b, k, and n are coefficients*

The equilibrium moisture content in the material (M_e) was defined by the equation below (Adesola and Satimehin, 2014, Kien et al., 2024):

$$M_e = \left(-\frac{1}{0.1560}\right) ln\left[-\frac{(t_a-7.3988)}{190.44} ln(R_H/100)\right] \quad (2)$$

where:
t_a (°C) is drying air temperature;
R_H (%) is drying air humidity.

Drying rate (DR) is determined by the equation below:

$$\text{DR} = \frac{M_\tau - M_{(\tau+d\tau)}}{d\tau} \quad (3)$$

where:
$M_{(\tau+d\tau)}$ (d.b) is moisture content at time ‘‘τ + dτ”,
M_τ (d.b) is moisture content at time ‘‘τ”
dτ is the time difference.

The experimental data of MR versus τ was used for nonlinear regression analysis corresponding to the thin layer drying models chosen by SPSS Statistics V22.0 software, 2022 (see Table 1).

The three output parameters of nonlinear regression including Standard Error of Estimate (SEE), Residual Sum of Squares (RSS) and the quadratic regression coefficient (R^2) were applied to determine the quality of fit to experimental data. The better goodness-of-fit has been achieved with the higher value of R^2 and the lower value of SEE and RSS.

The output parameters of nonlinear regression as SEE and RSS are defined as below:

$$\text{SEE} = \sqrt{\frac{\sum_{i=1}^{n}(M-M_S)^2}{df}} \quad (4)$$

$$\text{RSS} = \sum_{i-1}^{n}(M - M_S)^2 \quad (5)$$

where:
M_s is the simulated value of M,
df is the degree of freedom
n is the number of data points.

Determination of Effective Moisture Diffusivity and Activation Energy

Moisture diffusion within the material is a drying kinetic parameter that determines the rate of moisture transfer from inside of the material to the surface (Beigi, 2016). One dimensional diffusion is assumed and Fick's diffusion equation is used for the analyzation of the only diffusion based thin layer drying equation (Demiray and Tulek, 2012).

The assumptions used for the analytical solution of effective moisture diffusivity model are as follows:
– Initial moisture content is uniformly distributed within the material,
– Mass transfer is symmetrical to the center of the slab,
– The moisture content at the surface of the material reaches the equilibrium moisture content instantaneously at the beginning of the drying process,
– Mass transfer is based on diffuse mechanism,
– The diffusion coefficient is constant,
– The shrinkage of material is negligible

Based on the assumptions above, equation (6) is derived from the theoretical model for defining diffusivity for slab geometry (Alibas, 2014).

$$\mathrm{LnMR} = Ln\frac{8}{\pi^2} - \left(\frac{\pi^2 D_{\mathrm{eff}}}{4.L^2}\right).\tau \tag{6}$$

where:
D_{eff} is effective moisture diffusivity within material, ($m^2 \cdot s^{-1}$)
L is the half of slab thickness, (m)
τ is the drying time, (s)

The plot of LnMR versus τ forms a straight line and the effective diffusivity (D_{eff}) is determined based on its slope (X_1) as below:

$$X_1 = -D_{eff}\left(\frac{\pi}{2L}\right)^2 \tag{7}$$

Activation energy is determined based on Arrhenius equation as below:

$$D_{\mathrm{eff}} = D_0 e^{\left(-\frac{E_a}{RT_a}\right)} \tag{8}$$

where:
D_o ($m^2 \cdot s^{-1}$) is the diffusivity constant,
T_a (K) is the absolute drying air temperature,
E_a (kJ mol^{-1}) is the activation energy
R is the universal gas constant (R = 8.3143 kJ·mol^{-1} K^{-1}).

Next, log natural is taken to equation (8) to obtain equation (9).

$$\mathrm{LnD}_{eff} = \left(-\frac{E_a}{R}\right)\frac{1}{T_a} + LnD_0 \tag{9}$$

Equation (9) is then solved to define the activation energy. In it, the plot of LnD_{eff} versus $1/T_a$ forms a straight line with slope (X_2). The activation energy is determined by equation (10).

$$X_2 = -\frac{E_a}{RT_a} \tag{10}$$

Results and Discussion

Dehydration Kinetics of Thin Layer Drying of Yam Process

In thin-layer drying of yam slices by the IR-assisted heat pump drying process, the change in moisture ratio (MR) versus drying time (τ) during the drying process is presented graphically in Figure 3. Figure 3 shows that the change in moisture ratio during the drying process, corresponding to all drying modes, tended to be similar. The increase in temperature and IR power accelerated moisture removal. As a result, drying time was shortened.

At the same temperature, the drying time was shorter at higher IR power. At a drying temperature of 50°C and IR power of 350 W, drying time was the shortest, reduced by 28% and 41% compared to IR power levels of 300 W and 250 W, respectively. Likewise, at temperatures of 40°C and 45°C, the drying time at higher IR power was shorter than at lower IR power. At a drying temperature of 45°C and IR power of 350 W, drying time was reduced by 25% and 36% compared to 300 W and 250 W, respectively. At 40°C and 350 W, drying time was reduced by 18% and 30% compared to 300 W and 250 W, respectively.

This can be explained by the IR heating mechanism, in which infrared electromagnetic radiation causes molecules within the material to vibrate at high frequency. This vibration leads to friction between the molecules, generating internal heat within the material (Fasina et al., 2001; Dan et al., 2021). As a result, the heating rate increases, enhancing moisture diffusion within the material, reducing the moisture ratio, and shortening the drying time (Onwude et al., 2019; Qu et al., 2019; Wu et al., 2019; Kien et al., 2024).

The plot of the drying rate (DR) versus moisture content is presented graphically in Figure 4. As shown in Figure 4, the drying rate was higher at higher moisture content of the drying material. This occurred during the initial stage of the drying process. Then, the drying rate gradually decreased as the moisture content of the material decreased. The drying rate continued to decline until the material's moisture content reached the equilibrium moisture value. At that point, the moisture content no longer decreased, or decreased only slightly and insignificantly. At this stage, the thin-layer drying process was considered complete.

Higher drying temperature and higher IR power significantly improved the drying rate compared to lower temperature and lower IR power. The characteristics of the drying rate versus moisture content observed in this experimental drying process were consistent with previous studies (Manuel et al., 2019; Le et al., 2022).

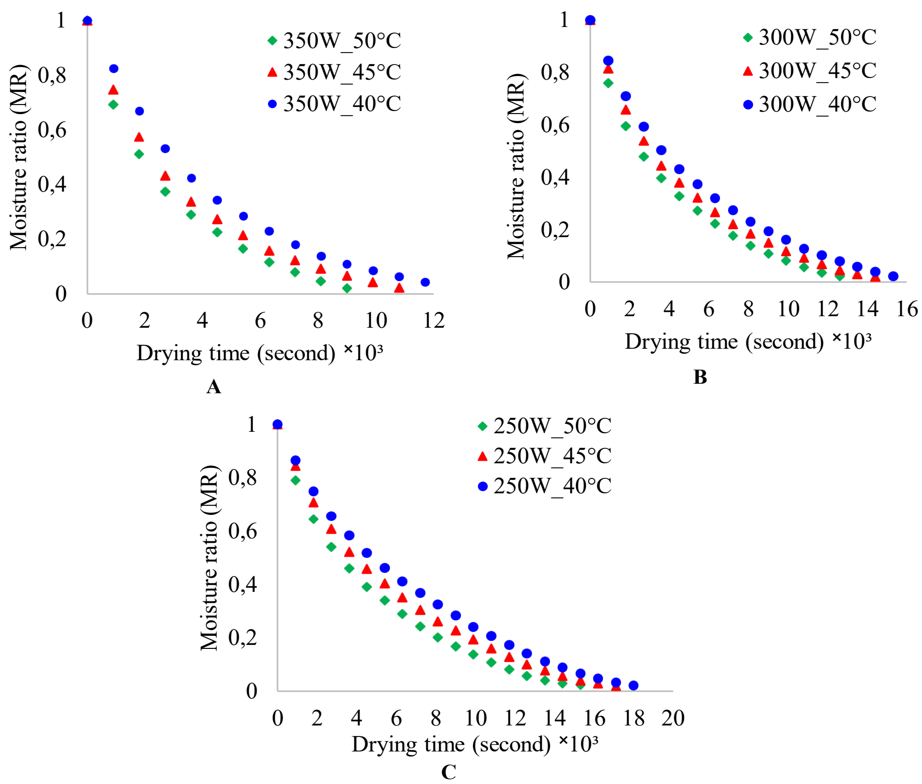

Figure 3. MR versus drying time at IR power of 350 W (A), 300 W (B) and 250 W (C)

The process of thin-layer drying of yam slices by IR-assisted heat pump appeared to occur exclusively in the falling-rate period, while the constant-rate period was rarely observed or was very difficult to detect in the thin-layer drying process. This was likely due to the extremely rapid removal of surface moisture from the yam slices (Correia et al., 2015; Abhishek et al., 2019; Le et al., 2022).

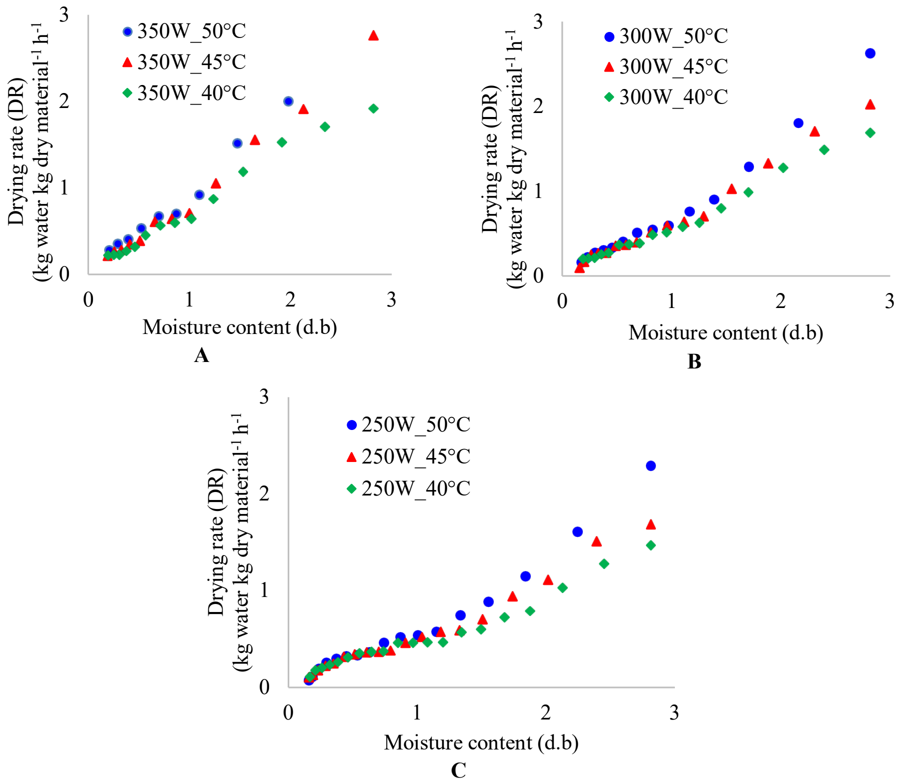

Figure 4. Drying rate versus moisture content at IR power of 350 W (A), 300 W (B) and 250 W (C)

The Statistical Evaluation of the Experimental Data For Determining the Best Fit Drying Model

The nonlinear regression analysis using SPSS Statistics software was conducted to determine the quality of fit to the experimental data (MR versus τ) according to the selected thin-layer drying models (see Table 1). The results for three statistical parameters are presented in Table 2. As shown in Table 2, the statistical parameters SEE and RSS had the lowest values, while R^2 had the highest value for the Midilli model across all drying modes. This result indicates that the Midilli model provided the best fit to the experimental thin-layer drying data.

Table 2.
Statistical parameters value of nonlinear regression analysis.

Models	Temperature (°C)	IR power of 250 W			IR power of 300 W			IR power of 350 W		
		R^2	RSS	SEE	R^2	RSS	SEE	R^2	RSS	SEE
Lewis	40	0.993	0.011	0.024	0.998	0.003	0.014	0.998	0.002	0.012
	45	0.996	0.006	0.018	0.998	0.003	0.014	0.999	0.001	0.011
	50	0.995	0.007	0.020	0.996	0.005	0.019	0.997	0.003	0.017
Page	40	0.994	0.010	0.023	0.998	0.003	0.014	0.999	0.001	0.008
	45	0.996	0.006	0.019	0.998	0.003	0.014	0.999	0.001	0.010
	50	0.996	0.005	0.018	0.9967	0.003	0.015	0.998	0.002	0.015
Modified Page	40	0.993	0.011	0.024	0.998	0.003	0.015	0.998	0.002	0.013
	45	0.996	0.006	0.019	0.998	0.003	0.014	0.999	0.001	0.011
	50	0.995	0.007	0.021	0.996	0.005	0.019	0.992	0.121	0.116
Henderson and Pabis	40	0.993	0.011	0.024	0.998	0.003	0.015	0.999	0.002	0.012
	45	0.996	0.006	0.019	0.998	0.003	0.014	0.999	0.001	0.011
	50	0.996	0.006	0.019	0.997	0.004	0.017	0.997	0.003	0.017
Wang and Singh	40	0.987	0.022	0.034	0.984	0.023	0.038	0.988	0.015	0.034
	45	0.979	0.033	0.043	0.975	0.033	0.047	0.974	0.028	0.051
	50	0.965	0.048	0.055	0.964	0.042	0.057	0.968	0.030	0.057
Midilli	40	0.999	0.001	0.006	0.999	0.0005	0.006	0.999	0.0004	0.006
	45	0.999	0.001	0.007	0.999	0.001	0.007	0.999	0.0003	0.006
	50	0.999	0.0005	0.006	0.999	0.0003	0.005	0.999	0.0003	0.006

Effective Moisture Diffusivity and Activation Energy

The value of effective moisture diffusivity (D_{eff}) and activation energy (E_a) were defined based on the slope of equation (7), and equation (10). They are given in Table 4.

Table 4.
Values of effective moisture diffusivity and activation energy

Specification `	Temperature (°C)	IR power (W)		
		250	300	350
Effective moisture diffusivity ($\times 10^{-9}$ $m^2 \cdot s^{-1}$) **	40	4.184	5.051	6.669
	45	4.750	5.656	7.381
	50	5.372	6.313	8.142
Activation energy ($kJ \cdot mol^{-1}$)		21.01	18.75	16.78

*** Significant at the 0.001 probability level ($p < 0.001$)*

In this study, ANOVA (Analysis of Variance) was used to compare the means of data. The P-value is based on F-distribution and represents the probability of observing the difference in theory and experiment. In the analysis, the effective moisture diffusivity was significant at the 0.001 probability level ($p < 0.001$), which indicates a very high level of statistical significance. This means there is less than a 0.1% chance that the observed results occurred purely by random variation.

As shown in Table 4, the effective moisture diffusivity of yam increased with rising drying temperature and IR power. This can be explained by the fact that increasing drying temperature and IR power enhanced heat exchange between the drying material and the drying air. At the same time, the internal heat generated by the IR heating mechanism also increased, thereby supporting the process of moisture diffusion within the yam. The effective moisture diffusivity of yam ranged from 4.184×10^{-9} to 8.142×10^{-9} $m^2 \cdot s^{-1}$, corresponding to drying temperatures from 40 to 50°C and IR power levels from 250 to 350 W. This result is consistent with previous studies on moisture diffusivity values for foods and vegetables (Bhattacharya et al., 2015; Motevali et al., 2016; Abhishek et al., 2019; Abhishek et al., 2020; Soner et al., 2020; Le et al., 2022).

The activation energy of moisture within yam was lower at higher IR power. The activation energy values were 16.78, 18.75, and 21.01 $kJ \cdot mol^{-1}$, corresponding to IR power levels of 250, 300, and 350 W, respectively. These values are consistent with previous studies on activation energy in food and vegetable drying (Bhattacharya et al., 2015; Motevali et al., 2016; Abhishek et al., 2019; Abhishek et al., 2020; Soner et al., 2020; Le et al., 2022).

The influence of IR power on activation energy is based on the IR heating mechanism. As the material absorbs more IR radiation, greater internal heat is generated. At that point, the water molecules within the material vibrate more rapidly, causing the bonds between them to weaken and become more easily broken.

The values of effective moisture diffusivity were fitted to the Arrhenius equation as a function of temperature, and the corresponding effective moisture diffusivity models for yam are presented in Table 5.

Table 5.
Effective moisture diffusivity model under different drying models.

IR power (W)	The effective moisture diffusivity model D_{eff} ($m^2 \cdot s^{-1}$)
250	$D_{eff} = 1.342 \times 10^{-5} \times Exp\left(-\frac{2527}{(t_a + 273.2)}\right)$
300	$D_{eff} = 6.795 \times 10^{-6} \times Exp\left(-\frac{2255}{(t_a + 273.2)}\right)$
350	$D_{eff} = 4.208 \times 10^{-6} \times Exp\left(-\frac{2018}{(t_a + 273.2)}\right)$

where: t_a (°C) is the drying temperature

Conclusion

1. The experimental thin-layer drying of yam slices by IR-assisted heat pump drying was conducted to define the dehydration kinetics of the thin-layer drying process. The results confirmed that increasing the drying temperature and IR power could significantly enhance the drying rate and reduce the moisture ratio.
2. The experimental drying data showed that the thin-layer drying process of yam slices using IR-assisted heat pump drying appeared to occur exclusively in the falling-rate period. The Midilli model was found to be the most suitable for describing the thin-layer drying behavior of yam.
3. The effective moisture diffusivity and the activation energy of moisture within yam were determined under different drying modes. The effective moisture diffusivity was higher at elevated drying temperatures and higher IR power. It ranged from 4.184×10^{-9} to 8.142×10^{-9} $m^2 \cdot s^{-1}$, corresponding to drying temperatures from 40 to 50°C and IR power levels from 250 to 350 W. The activation energy decreased from 21.01 to 16.78 $kJ \cdot mol^{-1}$ as IR power increased from 250 to 350 W.
4. In this study, the drying air velocity was fixed, as its influence on the drying process was considered minimal. However, to evaluate the impact of this parameter more comprehensively, future studies will vary the drying air velocity within a specified range.

Author Contributions: Conceptualization, P.V.K. and L.A.D.; methodology, P.V.K., L.A.D. and N.H; software, N.T.T. and D.Q.C; formal analysis, P.V.K. and L.A.D.; investigation, P.V.K. and L.A.D.; resources, P.V.K., L.A.D. and N.H; data curation, P.V.K., L.A.D. and N.H; writing—original draft preparation, P.V.K. and L.A.D.; supervision, P.V.K. and L.A.D. All authors have read and agreed to the published version of the manuscript.

Conflicts of Interest: The authors declare no conflict of interest.

Funding: This research was funded by Van Lang University, Ho Chi Minh City, Vietnam based on the decision No. 1606 of the President of Van Lang University, Ho Chi Minh City, Vietnam.

Acknowledgments: The authors would like to thank Van Lang University, Ho Chi Minh City, Vietnam and Nong Lam University, Ho Chi Minh City, Vietnam for funding this work.

References

Abbaspour, G.Y., Jahanbakhshi, A. & Kaveh, M. (2019a). Prediction kinetic, energy, and exergy of quince under hot air dryer using ANNs and ANFIS. *Food Science and Nutrition, 8*(1), 594-611.

Abhishek, D., Ramakrishna, K. & Naveen, P. (2019). Experimental investigation and mathematical modeling of convective drying kinetics of white radish. *Frontiers in Heat and Mass Transfer (FHMT), 13*, pp. 21.

Abhishek, D., Tarun, P., Ramakrishna, K. & Naveen, P. (2020). Convective hot air-drying kinetics of red beetroot in thin layers. *Frontiers in Heat and Mass Transfer (FHMT), 14*, pp. 23.

Adebimpe, F.O., Charles, T.A. & Tunde, A.M. (2021). Modeling of Thin Layer Drying Characteristics of Blanch-Assisted Water Yam (Dioscorea Alata) Slices. *Croatian Journal of Food Science and Technology, 13*(1), 43-50.

Adesola, A. & Satimehin, A. (2014). Mathematical Model for Deep Bed Drying of Gelatinized White Yam (Dioscorea rotundata, Poir). *International Journal of Energy Engineering, 4*(2A), 3pp. 3-39.

Akoy, E.O. (2014). Experimental characterization and modeling of thin-layer drying of mango slices. *International Food Research Journal, 21*(5), 1911-1917. https://www.researchgate.net/publication/273061769

Alibas, I. (2014). Mathematical modeling of microwave dried celery leaves and determination of the effective moisture diffusivities and activation energy. *Journal of Food Science and Technology, 34*(2), 394-401.

Behera, G. & Sutar, P.P.A (2018). Comprehensive review of mathematical modeling of paddy parboiling and drying: Effects of modern techniques on process kinetics and rice quality. *Trends in Food Science & Technology, 75*, 206-230.

Beigi, M. (2016). Hot air drying of apple slices: dehydration characteristics and quality assessment. *Journal of Heat and Mass transfer, 52*(8), 1435-1442.

Bhattacharya, M., Srivastav, P.P. & Mishra, H.N. (2015). Thin-layer modeling of convective and microwave-convective drying of oyster mushroom (Pleurotus ostreatus). *Journal of Food Science Technology, 52*(4), 2013-2022.

Chineze, G., Okeke, B.E., Eje, P.C. & Eze, I. (2020). Drying Characteristics of Yam Varieties: A Comparative Analysis. *Agricultural Engineering, 45*(1), 20–37.

Correia, A.F.K., Loro, A.C., Zanatta, S., Spoto, M.H.F. & Vieira, T.M.F.S. (2015). Effect of temperature, time and material thickness on the dehydration process of tomato. *International Journal of Food Science,* pp. 970724.

Dan, H., Pei, Y., Xiaohong, T., Lei, L. & Bengt, S. (2021). Application of infrared radiation in the drying of food products. *Trends in Food Science & Technology, 110*, 765–777.

Demiray, E. & Tulek, Y. (2012). Thin-layer drying of tomato (Lycopersicum esculentum Mill. cv. Rio Grande) slices in a convective hot air dryer. *Journal of Heat and Mass transfer,* 48(5), 841–847.

Egbe, E.W. (2022). Effect of Temperature on Dehydration Kinetics of Pre-Treated and Untreated Yam (Dioscorea spp) Slices. *Saudi Journal of Engineering and Technology*, 7(1), 1-10.

Fakhreddin, S. (2020). Recent Applications and Potential of Infrared Dryer Systems for Drying Various Agricultural Products: A Review. *International Journal of Fruit Science, 20*(3), 586-602.

Fakhreddin, S. (2021). Recent applications of heat pump dryer for drying of fruit crops: A Review. *International Journal of Fruit Science,* 21, 546–555.

Fasina, O., Tyler, B., Pickard, M., Zheng, G.H. & Wang, N. (2001). Effect of infrared heating on the properties of legume seeds. *International Journal of Food Science and Technology, 36*(1), 79-90.

John, O.O., Clinton, E.O., Abiola J. A., Oladayo A., Abiola F. O., Nana E. G. & Adeniyi, T. O. (2020). Drying characteristics of yamslices (Dioscorear otundata) in a convective hotairdryer: application of ANFIS in the prediction of drying kinetics. *Helyon*, *6*, pp. e03555.

Kai, N.S., Ai Mei, L., Fan, Z., Kiran, T., Jian, G.Z., Ji, H.H. & Zhao, J.W. (2019). Microstructural, Textural, Sensory Properties and Quality of Wheat–Yam Composite Flour Noodles. *Foods,* 8(10), pp. 519.

Kartik, S., Ramandeep, K., Satish, K., Ramesh, K.S., Surabhi, S., Subhash, V.P.& Vikas, K. (2023). Saponins: A concise review on food related aspects, applications and health implications. *Food Chemistry Advances, 2*, pp. 100191.

Kaveh, M., Jahanbakhshi, A., Abbaspour G.Y., Taghinezhad, E. & Moghimi, M.B.F. (2018). The effect of ultrasound pre-treatment on quality, drying, and thermodynamic attributes of almond kernel under convective dryer using ANNs and ANFIS network. *Journal of Food processing engineering, 41*, 123-134.

Keneni, Y.G., Hvoslef-Eide, A.K. & Marchetti, J.M. (2019). Mathematical modelling of the drying kinetics of Jatropha curcas L. seeds. *Industrial crops and products,* 132, 12-20.

Kien, P.V., Tan, N.T., Nghia, P.H., Tinh, V. N., Duc, L.A. & Hay, N. (2024). Heat and mass transfer in infrared assisted heat pump drying of purple yam. *Agricultural Engineering, 28*(1), 7 1-84.

Koua, K., Fassinou, W., Gbaha, P. & Toure, S. (2009). Mathematical modelling of the thin layer solar drying of banana, mango and cassava. *Energy, 34*, 1594-1602.

Le, A.D., Hay, N. & Kien, P.V. (2022). Mathematical model of thin layer drying of ganoderma lucidum by radio frequency assisted heat pump drying. *Frontiers in Heat and Mass Transfer (FHMT), 18*(44), 1-7.

Le, A.D., Kien, P.V., Tan, N.T., Son, D.T., Nhanh, V.N. & Ngoc, X. N. (2023). Heat and mass transfer in drying of carrot by radio frequency assisted heat pump drying. *Frontiers in Heat and Mass Transfer (FHMT),* 20, pp. 25.

Linlin, L., Min, Z. & Bhesh, B. (2019). Influence of drying methods on some physicochemical, functional and pasting properties of Chinese yam flour. *LWT - Food Science and Technology, 111*, 182-189.

Liu, Z., Bia, J., Wang, S., Meng, J., Wang, H., Yu, X., Gao, Z. & Xiao, H. (2019). Prediction of energy and exergy of mushroom slices drying in hot air impingement dryer by an artificial neural network. *Drying Technology, 38*(15), 1959-1970.

Manuel, C., María, L.M.C., Luis, P.V., Lucía, H., Juan, F.G.M. & Sebastián, S. (2019). Drying kinetics and effective water diffusivities in olive stone and olive-tree pruning. *Renewable Energy, 132*, 911-920.

Midilli, A. & Kucuk, H. (2003). Mathematical modelling of thin layer drying of pistachio by using solar energy. *Energy Conversion and Management, 44*(7), 1111-1122.

Mostafa, K.Md., Rahmat, A.Md., Mohammad, Rezaul, I.S. & Shakti, C.M. (2020). Thin-layer drying kinetics of yam slices, physicochemical, and functional attributes of yam flour. *Food Process Engineering,* 2020, pp. e13448.

Motevali, A., Saeid, M., Ahmad, B., Barat, G. & Hosain, D. (2016). Energy analyses and drying kinetics of chamomile leaves in microwave-convective dryer. *Journal of the Saudi Society of Agricultural Sciences, 15*(2), 179-187.

Nidhal, B.K. (2018). Effect of the variability of heat and mass transfer coefficients on 3D unsaturated porous medium drying. *Frontiers in Heat and Mass Transfer (FHMT),* 10, pp. 28, 1-7.

Nurdi, S., John, S.M., Saka, S. & Yoshiharu, F. (2021). Variation in the Physical and Functional Properties of Yam (Dioscorea spp.) Flour Produced by Different Processing Techniques. *Foods, 10*(6), pp. 1341.

Olatoye, K.K. & Arueya, G.L. (2019). Nutrient and phytochemical composition of flour made from selected cultivars of aerial yam (Dioscorea bulbifera) in Nigeria. *Journal of Food Composition and Analysis,* 79, 23-27.

Omari, A., Behroozi K.N. & Sharifian, F. (2018). Drying kinetics and artificial neural network modeling of the mushroom drying process in a microwave-hot air dryer. *Journal of Food Processing Engineering, 41*(7), pp. e12849.

Ononogbo, C. & Nwakuba, N.R., Nwaji, G.N., Nwufo, O.C., Nwosu, E.C., Okoronkwo, C.A., Igbokwe, J.O., Anyanwu, E.E. (2022). Thermal efficiency and drying Behaviour of Yam slices in a dryer driven by the waste heat of exhaust gases. *Scientific African, 17*, pp. (e01310) 1-11.

Onwude, D.I., Hashim, N., Abdan, K., Janius, R. & Chen, G. (2019). The effectiveness of combined infrared and hot-air drying strategies for sweet potato. *Journal of Food Engineering,* 241, 75-87.

Qu, F., Zhu, X., Ai, Z, Ai, Y., Qiu, F. & Ni, D. (2019). Effect of different drying methods on the sensory quality and chemical components of black tea. *LWT - Food Science and Technology,* 99, 112-118.

Rastogi, N.K. (2012). Recent trends and developments in infrared heating in food processing, *Critical Reviews in Food Science and Nutrition,* 52, 737-760.

Royen, M.J., Noori, A.W. & Haydary, J. (2020). Experimental Study and Mathematical Modeling of Convective Thin-Layer Drying of Apple Slices. *Processes*, *8*, pp.1562.

Salam, A., Aboud Ammar, B.A.A., Al-HiIphy, R. S., Lee, Y.C. & Francesco, C. (2019). A Comprehensive Review on Infrared Heating Applications in Food Processing. *Molecules, 24*(22), pp. 4125.

Soner, S. & Fatih, A. (2020). Experimental investigation of drying kinetics of apple with hot air, microwave and ultrasonic power. *Sadhana, 45*, 94-104.

Srikanth, K.S., Sharanagat, V.S., Kumar, Y., Bhadra, R., Singh, L., Nema, P.K. & Kumar, V. (2019). Convective drying and quality attributes of elephant foot yam (Amorphophallus paeoniifolius). *LWT - Food Science and Technology, 99*, 8-16.

Uwem, E.I., Innocent, O.O. & Benjamin, R.E. (2018). Kinetic Models for Drying Techniques—Food Materials. *Advances in Chemical Engineering and Science, 8*(2), 27-48.

Waheed, M.A. & Komolafe C.A. (2019). Temperatures dependent drying kinetics of cocoa beans varieties in air-ventilated oven. *Frontier in Heat and Mass Transfer (FHMT), 12*, pp. 8.

Wu, X.F., Zhang, M. & Bhandari, B. (2019). A novel infrared freeze drying (IRFD) technology to lower the energy consumption and keep the quality of Cordyceps militarist. *Innovative Food Science and Emerging Technologies, 54*(4), 34-42.

Zi, L.L., Long X., Magdalena, Z., Zhongli, P., Li Z.D., Jing, S.Z.L.G., Shan, Y.W., Zhi, A.Z. & Hong, W.X. (2022). Improvement of drying efficiency and quality attributes of blueberries using innovative far-infrared radiation heating assisted pulsed vacuum drying (FIR-PVD). *Innovative Food Science and Emerging Technologies,* 77, pp. 102948, 2022.

MATEMATYCZNY MODEL PROCESU SUSZENIA CIENKOWARSTWOWEGO IGNAMU FIOLETOWEGO ZA POMOCĄ POMPY CIEPŁA Z PROMIENIOWANIEM PODCZERWONYM

Streszczenie. Celem badania jest opracowanie modelu suszenia cienkowarstwowego ignamu fioletowego za pomocą pompy ciepła z promieniowaniem podczerwonym i określenie efektywnej dyfuzyjności wilgoci zawartej w fioletowym ignamie oraz energii jej aktywacji. Eksperyment suszenia cienkowarstwowego przeprowadzono przy następujących parametrach wejściowych: temperatury suszenia: 40, 45 i 50°C, prędkość powietrza suszącego: 2,5 $m \cdot s^{-1}$ a moc promieniowania podczerwonego: 250, 300 i 350 W. Aby określić taki model suszenia cienkowarstwowego, który opisywałby proces suszenia ignamu fioletowego przeprowadzono nieliniową regresję danych eksperymentalnych z wykorzystaniem sześciu różnych modeli suszenia cienkowarstwowego (Lewis, Page, zmodyfikowany Page, Henderson i Pabis, Wang i Singh oraz Midilli). Najbardziej odpowiednim modelem okazał się model Midilli. Średnia efektywna dyfuzyjność wilgoci w tym modelu mieściła się w zakresie od $4{,}184 \times 10^{-9}$ do $8{,}142 \times 10^{-9}$ $m^2 \cdot s^{-1}$, natomiast energia aktywacji wynosiła od 16,78 do 21,01 $kJ \cdot mol^{-1}$ w analizowanym zakresie parametrów suszenia.

Słowa kluczowe: szybkość suszenia, pompa ciepła, efektywna dyfuzyjność wilgoci, energia aktywacji, temperatura suszenia, moc promieniowania podczerwonego